

THE INFLUENCE OF APEX ANGLE ON MIXED CONVECTION IN A POROUS SECTOR CHANNEL

Manar Salih Mahdi

Department of Mechanical Engineering, College of Engineering, University of Tikrit

E-mail: manar_salih@yahoo.com

(Received: 18/10/2009; Accepted: 27/12/2010)

ABSTRACT: - The influence of apex angle on mixed convection in a horizontal porous sector channel is investigated. The analysis is performed by considering fully- developed hydrodynamically and thermally flow. The governing equations have been solved numerically using finite difference method. The channel is heated from the right surface, and cooled from the left one –both are held at constant temperature- while the top surface is adiabatic. The numerical analysis has been conducted in the following range of parameters: radius of the sector=4, (Pe=20), ($Ra^*=100$ and 1000), the apex angle ($\Phi=30^\circ$, 60° , 75° and 90°). The results are presented to demonstrate the effect of increasing the apex angle on the streamlines, the isotherms and local Nusselt number. The highest stream function appears in a specified apex angle depending on Ra^* . The local Nusselt number values are decreasing as the apex angle is increasing at ($Ra^*=1000$), while at ($Ra^*=100$) its values are increasing as the apex angle is increasing. A correlating equation is suggested to correlate (\overline{Nu}) against apex angle (Φ) and (Ra^*) for (Pe=20).

Keywords: - porous, mixed convection, horizontal sector channel.

NOMENCLATURE

a	Radius of the sector
g	Gravitational acceleration
k	Permeability of the porous medium
Nu	Local Nusselt number
\overline{Nu}	Average Nusselt number

THE INFLUENCE OF APEX ANGLE ON MIXED CONVECTION IN A POROUS SECTOR CHANNEL

p	Pressure
Pe	Peclet number ($\frac{\omega a}{\alpha}$)
r	Radial coordinate Dimensionless radial
R	coordinate ($\frac{r}{a}$)
Ra*	Rayleigh number for porous medium ($\frac{g \beta k a \Delta T}{\alpha \nu}$)
T	Temperature
u	Radial velocity component
v	Angular velocity component
Greek symbols	
α	Thermal diffusivity
θ	Dimensionless temperature ($\frac{T - T_c}{T_h - T_c}$)
μ	Viscosity
ρ	Density
Φ	Apex angle
φ	Angular coordinate
ψ	Stream function Dimensionless stream
Ψ	function ($\frac{\psi}{\omega a}$)
ω	Axial velocity component
Subscripts	
c	Cold
h	Hot

INTRODUCTION

Convective heat transfer in porous media has attracted a considerable attention over the last few decades because of its wide applications including geothermal energy engineering groundwater pollution transport, nuclear waste disposal, chemical reactors engineering, insulation of buildings and pipes, and solar power collectors^(1,2).

Badr and Pop (1988)⁽²⁾ had investigated numerically mixed convection heat transfer from a horizontal rod of a circular cross-section that is embedded in a porous medium for two cases, when the forced flow is directed either vertically upward or vertically downward. They solved the steady state problem by using the method of series truncation in combination with a finite-difference scheme. They used wide range of Reynolds number (5, 10, 20, 50 and 100) and Grashof number (0, 40, 80 and 400) for a Prandtl number of 0.7. Their study reveals that the boundary layer solutions to problems of this type give good results for most practical purposes even at low Grashof numbers. Their results show how the theories at both low and high Grashof numbers are approached. Also it was shown that applying such a method to this mixed convection problem not only provides much useful information about the physics of the flow phenomenon but also provides solutions which can be useful in future computational approaches.

Chang and Shiah (2005)⁽³⁾ presented numerical simulation ignores the nonlinear inertia terms of non-Darcian mixed convection in an isothermally horizontal channel with packed spheres (stainless sphere and water). Non-Darcian convection, including the no-slip boundary, flow inertia, channeling effect and thermal dispersion effect had been considered in the theoretical analysis. The ranges of the Rayleigh number ($Ra = 0 - 2 \times 10^5$), and the Peclet number ($Pe = 10 - 300$) were used in their study. To track accurately the near-wall porosity variation and the near-wall damping of dispersion conductivity, a non-uniform grid system was used. A numerical experiment was made to ensure the independence of the numerical results on the grid size and axial step. A secondary flow, induced by the buoyancy effect, occurred when Ra was high and Pe was low. They also found that the onset of the buoyancy effect occurred at a particular step in the thermally developing entrance region. The step depended on Rayleigh number. The local Nusselt number, would have no minimum unless the buoyancy effect is balanced by the thermal dispersion effect. However, the buoyancy effect was negligible for certain regions of the lower Ra (for example, $0 - 5 \times 10^3$). Further more they found that as the value of Pe was increasing (at the larger value $Pe = 300$ for $Ra =$

105 and $Pr = 10$), the thermal dispersion effect was induced and the buoyancy effect was also suppressed.

Bachok and Ishak (2009)⁽⁴⁾ had investigated theoretically the steady mixed convection boundary layer flow along a permeable vertical cylinder with prescribed surface heat flux. The free stream velocity and the surface heat flux were assumed to vary linearly with the distance from the leading edge. The governing system of partial differential equations was first transformed into a system of ordinary differential equations, then the transformed equations were solved numerically for both assisting and opposing flow regimes using two different methods, namely the Keller-box method and the NAG routine D02HAF.

They discussed the effects of the curvature parameter, suction or injection parameter and the buoyancy parameter on the skin friction coefficient and the surface temperature for $Pr = 1$. From their investigation they concluded that dual solutions exist also for the assisting flow; for the opposing flow there were dual solutions, unique solution or no solution; the solution curves bifurcate at the critical point; suction delayed the boundary layer separation, while injection accelerated it; finally they concluded that larger values of the curvature parameter (smaller values of the cylinder diameter) will delay the boundary layer separation.

Yadav et al. (2010)⁽⁵⁾ had investigated the time dependent thermal convection of a viscous, electrically conducting fluid through a porous medium in horizontal channel bounded by wavy walls. The imposed oscillatory flow on the convective flow through the channel caused the unsteadiness in the flow. The flow phenomenon was analyzed for different sets of the parameters Gr , Re , Hartmann Number, the coefficient of thermal expansion, and Wormsley number governing the flow. The coupled equations governing the flow and heat transfer were solved using a perturbation technique. They noticed that the flow was basically asymmetric due to distinct surface temperatures. The non-uniformity in the boundary gave rise to a secondary transverse flow and hence the general pattern of the flow can be judged by studying the individual velocity. They found that the primary velocity in a constricted channel was negative for all variations in the entire fluid region thereby indicating the reversal flow in the entire fluid region. Also they found that the secondary velocity in the lower half was towards the boundary and was towards the mid-plane in the upper half in the heating case while a reversed effect was noticed in the cooling case. Further more it was found that greater the constriction larger the temperature in the lower half and smaller non-dimensional temperature in the upper half while in a dilated case a reversed effect was noticed in the fluid region, the magnitude of the stress at both the walls decreased with increasing in Gr ; the rate of heat transfer was negative at both the walls for all variations; the magnitude of the Nusselt Number depreciated at both the walls

with increasing in Gr value and increased with increasing in Re or Hartmann Number, and an increasing Wormsley number would result an enhancement in Nu.

Nazar et al. (2010)⁽⁶⁾ had studied steady mixed convection boundary layer flow from an isothermal horizontal circular cylinder embedded in a porous medium filled with a nanofluid for both cases of a heated and cooled cylinder. They solved the governing non-similar boundary layer equations numerically using the Keller-box method along with the Newton's linearization technique. The solutions for the flow and heat transfer characteristics were evaluated for various values of the governing parameters, namely the nanoparticle volume fraction and the mixed convection parameter. Three different types of nanoparticles were considered, namely Cu, Al₂O₃ and TiO₂. It was found that for each particular nanoparticle, as the nanoparticle volume fraction increased, the magnitude of the skin friction coefficient decreased, and this leads to an increase in the value of the mixed convection parameter which first produces no separation. On the other hand, it was also found that of all the three types of nanoparticles considered, for any fixed values of the nanoparticle volume fraction and the mixed convection parameter, the nanoparticle Cu gave the largest values of the skin friction coefficient followed by TiO₂ and Al₂O₃. They mentioned that heating the cylinder would delay separation of the boundary layer and if the cylinder was hot enough, then it was suppressed completely. On the other hand, cooling the cylinder brings the boundary layer separation point nearer to the lower stagnation point and for a sufficiently cold cylinder there will not be a boundary layer on the cylinder.

One of the most basic problems in porous media which has important applications in many fields is convective heat transfer; To the author's knowledge the problem of mixed convection in a horizontal porous sector channel has received less attention ^(7, 8, 9). In this paper the effect of changing the apex angle on mixed convection in a porous sector channel is investigated numerically. the fluid is flowing steadily in a porous medium through impermeable horizontal channel. One surface is heated (T_h) and the other is cooled (T_c) where both of them at constant temperature, while the top surface is kept adiabatic.

PROBLEM FORMULATION

A horizontal sector channel filled with a fluid- saturated porous medium. The temperature of the right side of the sector assumed to be higher than the left side, and both of them are maintained at constant temperatures, while the top of the sector is adiabatic. The channel is subjected to mixed convection.

ASSUMPTIONS

In the porous media, the following assumptions are made:

1. The porous medium is homogeneous and isotropic.
2. Porosity is constant thought out of the medium.
3. No heat generation inside the porous medium.
4. Darcy and Boussinesq approximations are valid.
5. The end effects are neglected and the flow is assumed to be 2- dimensional.
6. Inertial effects are negligible due to small velocity of the fluid through the medium.
7. The convective fluid and the porous medium are in thermal equilibrium.
8. the viscosity of the fluid is low so the viscous dissipation effects are negligible.

MATHEMATICAL MODEL

The physical model and the coordinate system in the present analysis are shown in figure (1).

The conservation equations for mass, momentum and energy for a steady mixed convection flow in a porous medium can be written in polar co- ordinates (r, ϕ) as ⁽¹⁰⁾:

$$\frac{\partial u}{\partial r} + \frac{u}{r} + \frac{1}{r} \frac{\partial v}{\partial \phi} = 0 \quad (1)$$

Where $(\frac{\partial \omega}{\partial z} = 0)$ since the axial velocity (ω) is constant.

$$u = -\frac{k}{\mu} \left[\frac{\partial p}{\partial r} - \rho g \cos \phi \right] \quad (2)$$

$$v = -\frac{k}{\mu} \left(\frac{1}{r} \frac{\partial p}{\partial \phi} + \rho g \sin \phi \right) \quad (3)$$

$$\alpha \left[\frac{\partial^2 T}{\partial r^2} + \frac{1}{r} \frac{\partial T}{\partial r} + \frac{1}{r^2} \frac{\partial^2 T}{\partial \phi^2} \right] = u \frac{\partial T}{\partial r} + \frac{v}{r} \frac{\partial T}{\partial \phi} \quad (4)$$

Substituting Boussinesq approximation in equations (2 and 3) and by cross differentiation we get combined momentum equation, then the governing equations can be written in terms of stream function defined as $(u = \frac{1}{r} \frac{\partial \psi}{\partial \phi})$ and $(v = -\frac{\partial \psi}{\partial r})$, subsequent nondimensionalisation using:

$$R = \frac{r}{a}, \Psi = \frac{\Psi}{\omega a}, \theta = \frac{T - T_c}{T_h - T_c}$$

Leads to the following dimensionless form of the governing equations:

$$\frac{\partial^2 \Psi}{\partial R^2} + \frac{1}{R} \frac{\partial \Psi}{\partial R} + \frac{1}{R^2} \frac{\partial^2 \Psi}{\partial \varphi^2} = \frac{Ra^*}{Pe} \left[\frac{\cos \varphi}{R} \frac{\partial \theta}{\partial \varphi} + \sin \varphi \frac{\partial \theta}{\partial R} \right] \quad (5)$$

$$\frac{\partial^2 \theta}{\partial R^2} + \frac{1}{R} \frac{\partial \theta}{\partial R} + \frac{1}{R^2} \frac{\partial^2 \theta}{\partial \varphi^2} = \frac{Pe}{R} \left[\frac{\partial \Psi}{\partial \varphi} \frac{\partial \theta}{\partial R} - \frac{\partial \Psi}{\partial R} \frac{\partial \theta}{\partial \varphi} \right] \quad (6)$$

Equations (5) and (6) are subjected to the following non- dimensional boundary conditions:

$$\left. \begin{aligned} \Psi(1, \varphi) = 0.0, \quad \frac{\partial \theta(1, \varphi)}{\partial R} = 0.0 \\ \Psi(R, 0) = 0.0, \theta(R, 0) = 0.0 \\ \Psi(R, \Phi) = 0.0, \quad \theta(R, \Phi) = 1.0 \end{aligned} \right\} \quad (7)$$

The local Nusselt number along the hot side is given by:

$$Nu = \left. \frac{\partial \theta}{\partial \varphi} \right]_{\varphi=\Phi} \quad (8)$$

And the average Nusselt number is defined as:

$$\overline{Nu} = \int_0^1 Nu.dR \quad (9)$$

NUMERICAL SOLUTION

Equations (5) and (6) are subjected to the boundary conditions (7) and transformed into finite difference equations, solved numerically using a successive under relaxation procedure.

The solution started assuming that (Ψ) and (θ) in internal points are zero and by using Gauss- Seidl method new values of (Ψ) and (θ) are substituted, the relaxation factor chosen was (0.2) for both stream function and temperature.

Iterations are terminated when the relative error convergence criterion was satisfied:

$$\left| \frac{B^n - B^{n-1}}{B^{n-1}} \right| \leq 10^{-3}$$

Where (B) indicates the value of (Ψ) or (θ) at the nth step of the iteration.

RESULTS AND DISCUSSION

The influence of apex angle on mixed convection in a porous sector channel is investigated numerically using finite difference method. The flow is fully developed hydrodynamically and thermally. The numerical results have been obtained for ($Pe = 20$), ($Ra^* = 100$ and 1000) and apex angle ($\Phi = 30^\circ, 60^\circ, 75^\circ$ and 90°).

For low (Ra^*) ($Ra^* = 100$), left hand side of figures (2-5), the power of the stream function (the minus sign indicates anti-clockwise rotation) increases till it gets its highest value at ($\Phi = 60^\circ$), then the intensity of the stream function decreases as the apex angle increases, this happened due to decreasing the area of the hot and cold surfaces comparing with the upper adiabatic surface, which means lower heat mixing. The center of rotation moves from the upper half of the cavity (at $\Phi = 30^\circ$), to get to the center of the cavity at ($\Phi = 60^\circ$), then it heads toward the lower half closed to the cold surface, where a stagnation region is formed in the upper right corner near the hot surface because of increasing the thickness of the thermal boundary layer there.

The semi uniform isotherms at ($\Phi = 30^\circ$), right hand side of figures (2-5), means that the conduction still affecting upon heat transfer through the cavity, by increasing the apex angle the isotherms become more distorted indicating increasing the effect of convection in heat transfer. Converging isotherms in the lower region of the cavity near the hot surface indicates increasing in heat transfer and Nu in this part of the cavity, while diverging these isotherms in the upper region of the cavity near the hot surface indicates decreasing in heat transfer which is very expectant since the cold fluid running down from the cold surface (which is the coldest fluid in the cavity) is hitting the hot surface from below, which means high temperature difference and high heat transfer rate, the warm fluid rises beside the hot surface since its density is getting lower, its temperature also is increasing and the temperature difference between the fluid and the hot surface is decreasing, leading to lower heat transfer rate than in the lower part of the hot surface.

The lowest Nu appears at ($\Phi = 30^\circ$), figure (6), because of the conduction effects on heat transfer as mentioned above. Nu value increases as the convection effect increases, but as the apex angle is increasing, the area swept by the fluid along the hot and cold surfaces becomes smaller, leading to less heat convected by the fluid, and decreasing Nu . The same figure assures that the highest Nu along the hot surface is in the bottom of it, while lowest value of Nu is in the top of the hot surface.

As a result for increasing of (Ra^*) ($Ra^* = 1000$), left hand side of figures (7-10), the values of stream function are increasing to get it's highest value at ($\Phi = 75^\circ$), after that these values decrease because of decreasing the amount of convected heat through the cavity for decreasing the areas of the hot and cold surfaces comparing to the adiabatic one. The streamlines diverge in the upper and lower parts of the cavity due to thick thermal boundary layer, while these lines converge close to the hot and cold surfaces ($\Phi = 30^\circ$ and 60°), and close to the upper right corner and the cold surface ($\Phi = 75^\circ$ and 90°) because of the small thickness of the thermal boundary layer. The central core is constant and occupies most of the cavity center.

The isotherms, right hand side of figures (7-10), converge in the lower part of the cavity near the hot surface, and diverge in the upper region where the thickness of the thermal boundary layer increases. The isotherms highly distorted as the apex angle increase causing temperature inversion ($\Phi = 60^\circ, 75^\circ$ and 90°).

As shown in figure (11) the wide area of the hot and cold surfaces ($\Phi = 30^\circ$) has led to increasing the amount of the convected heat by the fluid through the cavity, which increases the value of Nu at this angle, but as apex angle increases the area of the hot and cold surfaces decreases, causing decreasing in Nu value. The highest Nu appears in the lower region of the cavity near the hot surface as a result of thin thermal boundary as the fluid rises along the hot surface, it's temperature increases (increasing the thickness of the thermal boundary layer) leading to smaller temperature difference between the fluid and the surface causing falling in Nu value along the hot surface to get it's lowest value in the upper region near the hot surface for all apex angles.

To have a clear understanding to the relationship between \overline{Nu} and both Ra and apex angle a correlating equation is suggested below:

$$\overline{Nu} = 0.58Ra^{0.61}(\sin \Phi)^{-0.19}$$

This correlation is valid for $Pe = 20$, $100 \leq Ra^* \leq 1000$ and, $30^\circ \leq \Phi \leq 90^\circ$, the maximum diverge of this correlation from the theoretical value is 18%.

CONCLUSIONS

At low Ra^* conduction may still affect the heat transfer through the cavity (depending on Ra^*) but by increasing the apex angle the convection will dominate the heat transfer.

One cell appears rotating in the anti-clockwise direction. The stream function increases as the apex angle increases then at a specified apex angle depending upon Ra^* the stream function will be weaker as the apex angle increases.

In the bottom of the hot surface the isotherms converge from each other more than in the upper of it indicating high heat transfer (Nu) in the bottom.

Any increasing in apex angle will reduces the convected heat from the hot surface to the cold one.

REFERENCES

1. Saeid, N. H. and Pop, I. , (2006), “Periodic mixed convection in horizontal porous layer heated from below by isoflux heater”, The Arabian Journal for Science and Engineering, Vol. 31, No. 2B, pp. 153-164.
2. Badr, H. M. and Pop, I., (1988), “combined convection from an isothermal horizontal rod buried in a porous medium”, Int. Journal of Heat Mass Transfer, Vol. 31, No. 12, pp. 2527-2541.
3. Chang, P. and Shiah, S., (2005), “Mixed Convection in an Isothermally Horizontal Channel with Packed Spheres”, Journal of C.C.I.T., Vol.33, No.2, pp.1-12.
4. Bachok, N. and Ishak, A., (2009), “Mixed Convection Boundary Layer Flow Over a Permeable Vertical Cylinder with Prescribed Surface Heat Flux”, European Journal of Scientific Research, Vol.34, No.1, pp. 46-54.
5. Yadav ,Y. R., Krishna, S. R., and Reddaiah, P., (2010), “Mixed Convective Heat Transfer Through a Porous Medium in a Horizontal Wavy Channel”, International Journal of Applied Mathematics and Mechanics, Vol. 6, No. 17, pp.25-54.
6. Nazar, R., Tham ,L., Pop, I., and Ingham, D. B., (2010), “Mixed Convection Boundary Layer Flow from a Horizontal Circular Cylinder Embedded in a Porous Medium Filled with a Nanofluid”, Transport in Porous Media, Online First™, [http://www.springerlink.com/content/?k=\(au%3a\(nazar+tham+pop\)\)+OR+ed%3a\(nazar+tham+pop\)\)](http://www.springerlink.com/content/?k=(au%3a(nazar+tham+pop))+OR+ed%3a(nazar+tham+pop))).
7. Vafai, K., (2005), “Hand Book Of Porous Media”, 2nd ed., Taylor & Francis, pp. 393-400.
8. Kaviany, M.,(1995) “Principles Of Heat Transfer In Porous Media”, 2nd ed., Springer, pp.157-254.

9. Nield, D. A., and Bejan, A., (1999), "Convection In Porous Media", 3rd ed., Springer, pp. 357-361.
10. Rasheed, S. A. H. , (2006), "Mixed Convection In Porous Media With Different Angle Of Inclination", (Ph. D. thesis in Arabic), University of Technology, pp. 31-32.

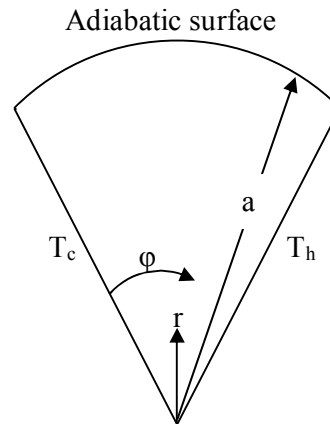


Fig. (1): physical model and the coordinate system.

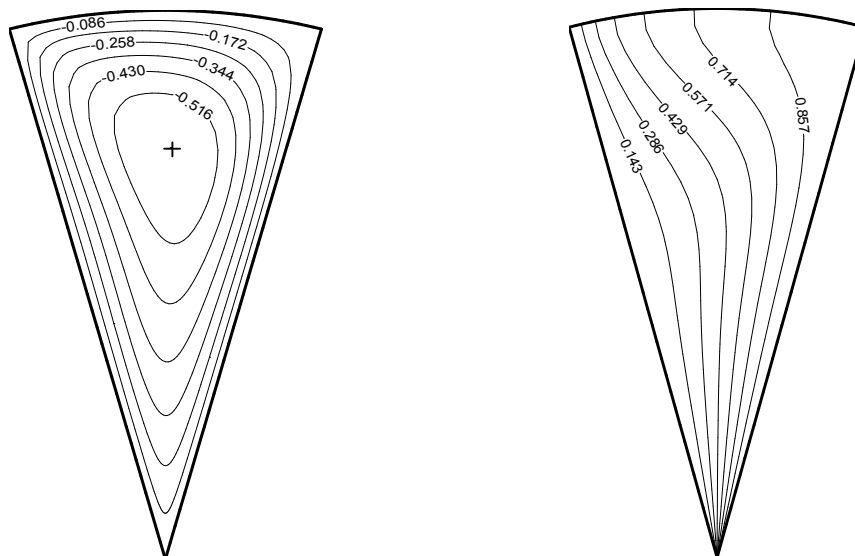


Fig. (2): Streamlines and isotherms for $Ra^* = 100$, $\Phi = 30^\circ$.

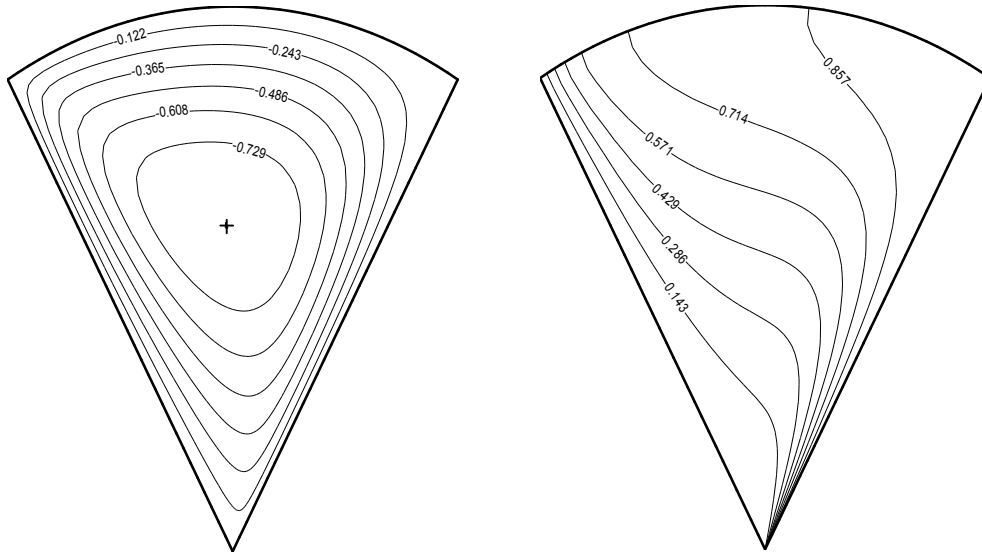


Fig. (3): Streamlines and isotherms for $Ra^* = 100, \Phi = 60^\circ$.

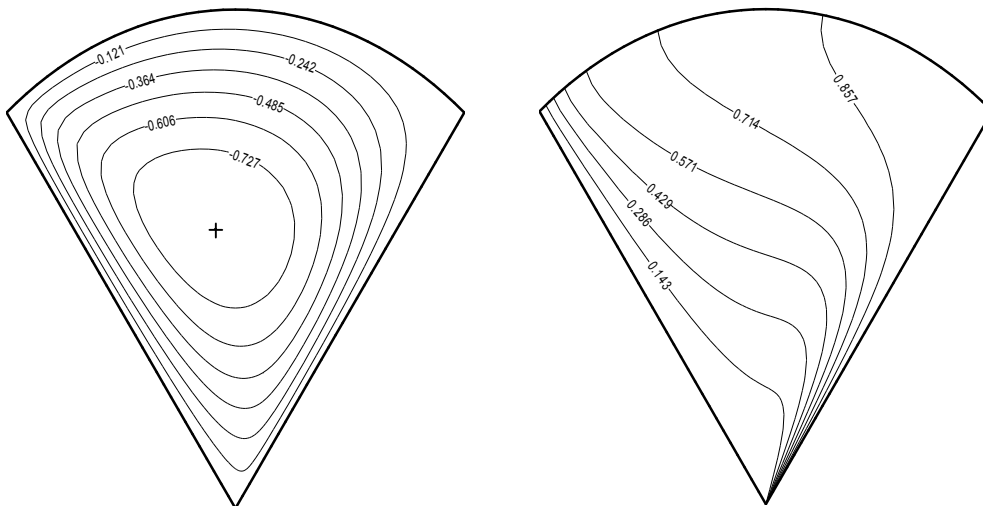


Fig. (4): Streamlines and isotherms for $Ra^* = 100, \Phi = 75^\circ$.

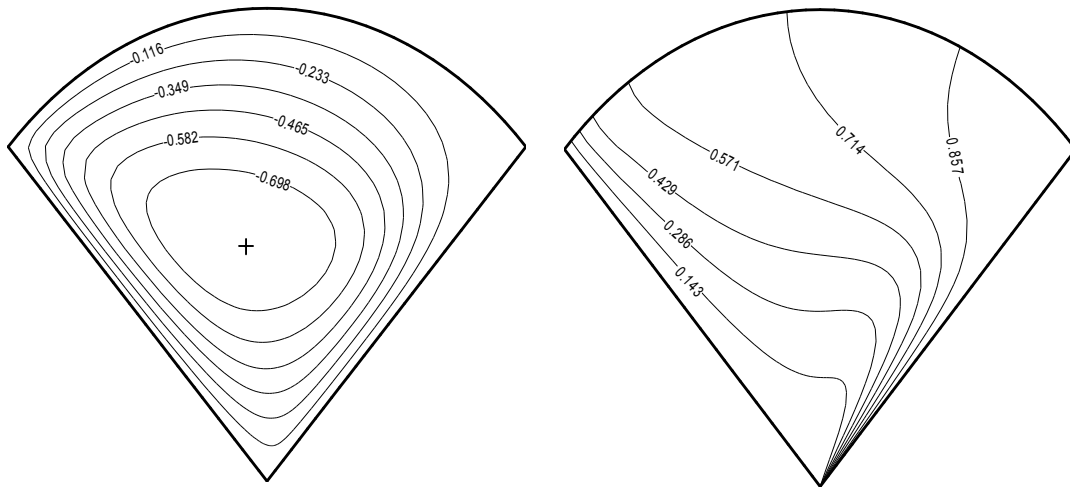


Fig.(5): Streamlines and isotherms for $Ra^*=100$, $\Phi=90^\circ$.

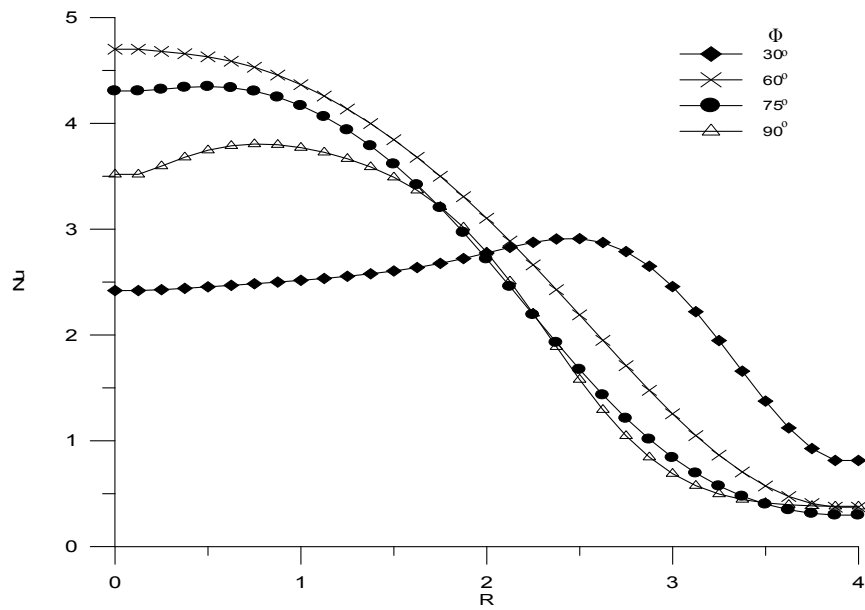


Fig. (6): Influence of apex angle on local Nusselt number at $Ra^*=100$.

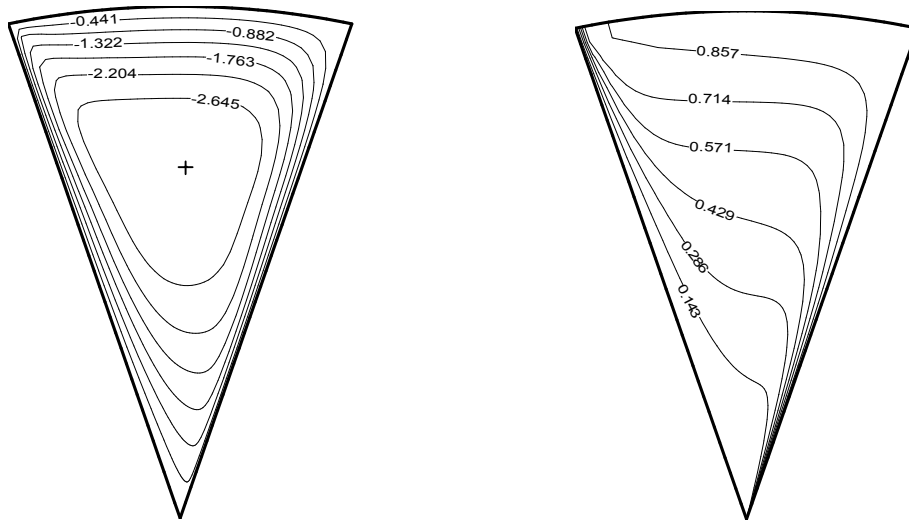


Fig.(7): Streamlines and isotherms for $Ra^* = 1000$, $\Phi = 30^\circ$.

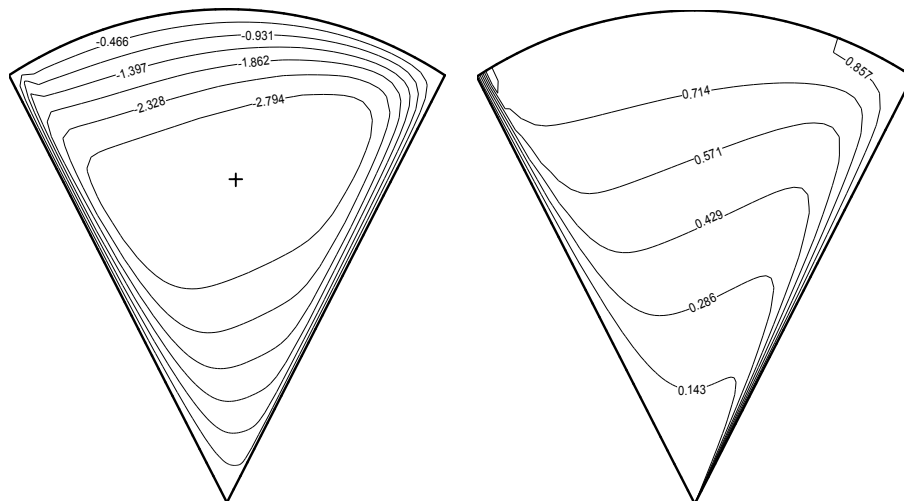


Fig.(8): Streamlines and isotherms for $Ra^* = 1000$, $\Phi = 60^\circ$.

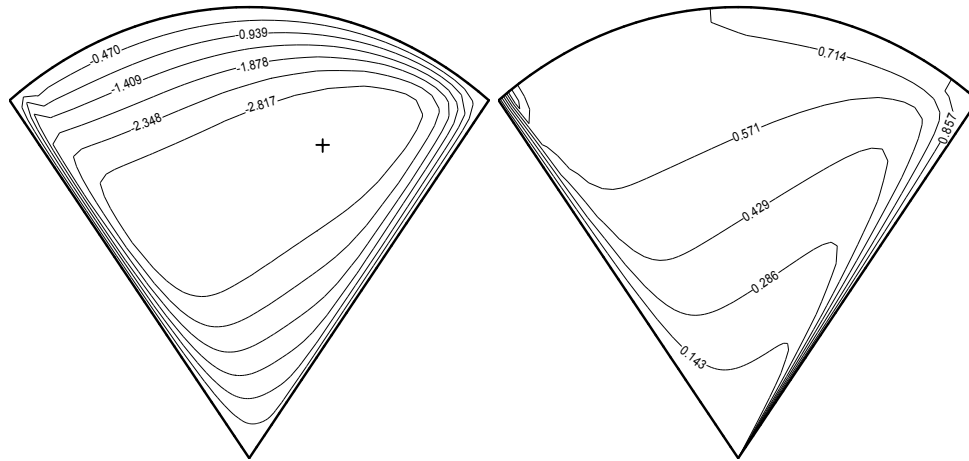


Fig.(9): Streamlines and isotherms for $Ra^* = 1000, \Phi = 75^\circ$.

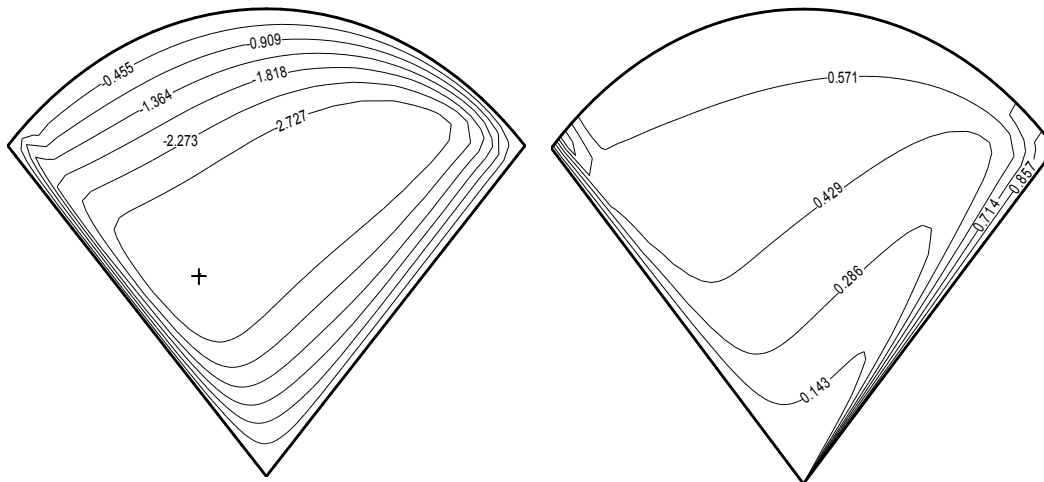


Fig. (10): Streamlines and isotherms for $Ra^* = 1000, \Phi = 90^\circ$.

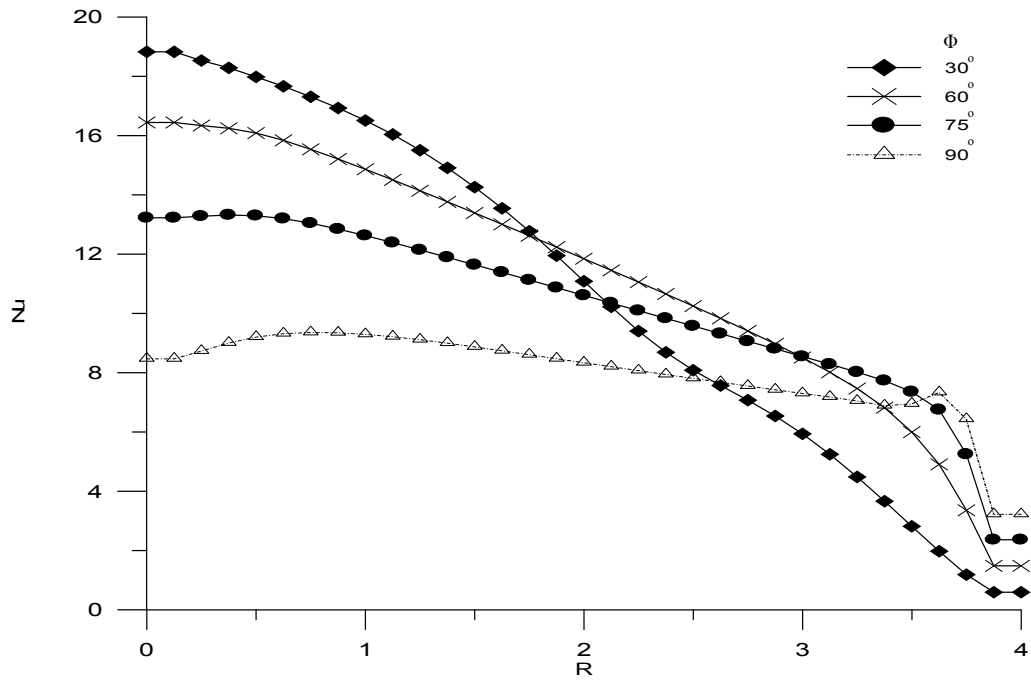


Fig. (11): Influence of apex angle on local Nusselt number at $Ra^*=1000$.

تأثير الزاوية الرأسية على الحمل المختلط في قناة مسامية قطاعية الشكل

منار صالح مهدي

مدرس مساعد

قسم الهندسة الميكانيكية - كلية الهندسة - جامعة

تكريت

الخلاصة

في هذا البحث تم استقصاء تأثير الزاوية الرأسية على الحمل المختلط في قناة أفقية مسامية قطاعية الشكل، أجريت التحليلات باعتبار الجريان تام التشكيل هيدروليكيًا وحراريًا، حلت المعادلات الحاكمة عددياً باستخدام طريقة الفروقات المحددة، سخن السطح الأيمن من القناة وبرد السطح الأيسر لها- كلاهما ثابتي درجة الحرارة-، بينما عزل السطح العلوي للقناة، أجريت التحليلات وفق المعاملات التالية: نصف قطر القطاع = 4، (Pe=20)، (Ra* = 100،)، الزاوية الرأسية (Φ=30°، 60°، 75°، و90°). وضحت النتائج تأثير زيادة الزاوية الرأسية على خطوط الجريان، خطوط ثبوت درجة الحرارة، وعدد نسلت الموقعي. تظهر أعلى قيمة لدالة الجريان عند زاوية رأسية معينة اعتماداً على قيم عدد (Ra*)، إن قيم عدد نسلت الموقعي تنخفض بزيادة الزاوية الرأسية عند (Ra*=1000) بينما عند (Ra*=100) تزداد قيمها بزيادة الزاوية الرأسية. أقترحنا علاقة ترابطية تربط معدل عدد نسلت (Nu) بالزاوية الرأسية (Φ) و (Ra*) عندما (Pe=20).
الكلمات الدالة: مسامي، حمل مختلط، قناة أفقية قطاعية الشكل.